33ND INTERNATIONAL COSMIC RAY CONFERENCE, RIO DE JANEIRO 2013
THE ASTROPARTICLE PHYSICS CONFERENCE

ICRC 2013

Spectrum and Morphology of the *Fermi* Bubbles

ANNA FRANCKOWIAK[1,2], DMITRY MALYSHEV[1,2], FOR THE *Fermi*-LAT COLLABORATION.

[1] *Kavli Institute for Particle Astrophysics and Cosmology*
[2] *SLAC National Accelerator Laboratory*

afrancko@slac.stanford.edu, malyshev@stanford.edu

Abstract: The *Fermi* bubbles are a spectacular remnant of a past activity in or around the Galactic center. They provide unique information about the history of the Milky Way and open a window into the gamma-ray study of similar extra-galactic objects. There are several theoretical models aiming to explain the origin of the bubbles. The morphology and the spectrum of the bubbles are derived from the residual maps after the subtraction of the foreground components. The foreground emission model used in this analysis is based on GALPROP (galactic propagation code).

Keywords: gamma-rays, diffuse background, Milky Way, AGN

1 Introduction

The *Fermi* bubbles are two large features in the gamma-ray sky extending up to 55 degrees above and below the Galactic center [16]. There are a handful of possible associations at low latitudes: ROSAT maps [17, 16], WMAP and Planck haze [18, 19, 20], and the detection of possibly related linearly polarized radio emission that extends to 60° [22]. The relative brightness in gamma-rays with a lack of strong counterparts in other frequencies makes the *Fermi* bubbles one of the most mysterious astrophysical objects.

While their origin is still unknown and debated, several theoretical models have been proposed to explain the formation of the bubbles and the gamma-ray emission mechanism. Provided that the bubbles are observed up to at least 100 GeV, the only possible emission mechanisms are hadronic [15] production of gamma-rays and inverse Compton scattering. For the hadronic scenario one expects to see some emission from the target material, i.e., gas, which is not observed at high latitudes. For the leptonic scenario one has to avoid the problem of cooling of leptons. Given the size of the bubbles and the characteristic cooling time, one has to either assume a supersonic expansion of the bubbles [13] or re-acceleration of the leptons inside the volume of the bubbles [14].

Different theoretical scenarios have different signatures in gamma-rays. For example, limb brightened emission with a harder spectrum near the edges supports scenarios where a strong jet from the central black hole [21] drives a supersonic expansion of a shock front. While volume-filling emission with a harder spectrum near the Galactic plane supports more continuous emission, such as strong winds from starbursts or a sequence of jets from the black hole. A featureless power-law spectrum at high energies is more common in hadronic emission scenarios, while cooling of leptons will manifest itself as a cutoff or significant softening at high energies.

The study of the *Fermi* bubbles is complicated by the existence of other emission components, such as the gamma-ray emission produced by Galactic cosmic rays propagating in the interstellar medium, the gamma-ray emission from LoopI (a nearby giant radio loop spanning centered on the Sco-Cen OB association [23]), extragalactic emission. The primary purpose of this work is to characterize their properties and morphology accounting for the uncertainties on the diffuse emission modeling.

2 Data Set

In the analysis we use 50 months of *Fermi*-LAT data between August 6, 2008 and October 7, 2012 (MET 239557448 - 371262668). We use the reprocessed Pass7 version 6 UltraClean event selection and instrument response functions to reduce the cosmic-ray background contribution. To minimize the contribution from the bright Earth limb, we apply a maximum zenith angle cut of $< 90°$. In addition, we also limit our data set to include only photons with an incidence angle from the instrument z-axis of $< 72°$. Exposure maps and the point spread function (PSF) for the pointing history of the observations were generated using the standard *Fermi*-LAT ScienceTools package available from the *Fermi* Science Support Center[1].

The *Fermi* bubbles have no known counterparts at high latitudes. Consequently, the derivation of the properties of the *Fermi* bubbles has to rely on the gamma-ray data itself. This is one of the main difference of the *Fermi* bubbles from the other emission components, such as the hadronic, the bremsstrahlung, the inverse Compton scattering (ICS) and the LoopI which can be estimated with the help of various tracers.

As a result, the general strategy of the data analysis related to the *Fermi* bubbles proceeds along the following steps:

- Construct a diffuse emission model that includes the hadronic, ICS, isotropic, and bremsstrahlung components, and LoopI.
- Use the residual maps obtained by subtracting the model from the data to model the template for the *Fermi* bubbles.
- Study the properties of the *Fermi* bubbles using the template derived in the previous step.

1. `http://fermi.gsfc.nasa.gov/ssc/data/analysis/`

3 Method

In order to extract the *Fermi* bubbles from the *Fermi*-LAT data we use the all-sky fitting tool GaDGET [1] which was developed and successfully applied to derive the spectrum of the isotropic diffuse gamma-ray emission [2]. GaDGET simultaneously fits the different components of the diffuse Galactic emission to the data in a maximum likelihood procedure.

3.1 Templates

The interstellar emission is modeled using the GALPROP code ([3, 4, 6, 5, 7, 8] and references therein). GALPROP calculates gamma-ray emissivities using the propagated CR spectra and intensities folded with the appropriate target distributions included in the GALPROP code: HI, H2, and HII gas distributions for π^0-decay and bremsstrahlung, and the interstellar radiation field for ICS. Gamma-ray intensity skymaps are obtained by direct line-of-sight integration of the calculated gamma-ray emissivities and are used as templates in the fit with free normalization in each energy bin. The gas-related gamma-ray intensities are computed in Galactocentric rings. The rings can be treated as separate templates in the fit reducing the uncertainty in the assumed cosmic ray density.

Bright point sources from the 2FGL catalog [9] , which have a test statistic above 200 are included with the flux per energy band per source as a fit parameter. Weaker sources are included with fluxes derived from the 2FGL catalogue analysis. In addition the emission of LoopI is included according to a geometrical template described in [12]. This geometrical model is based on a polarization surveys at 1.4GHz and explains the observed emission by synchrotron emission from two expanding gas shells. Finally, a template for the bubbles is derived and included in the fit. The definition of the bubble template is described below.

Gamma-ray skymaps were generated using a HEALPix [10] isopixelisation scheme at order 6 ($\sim 1.0^\circ$ resolution) with 25 logarithmical spaced independent energy bins from 100 MeV to 500 GeV. The GALPROP flux maps are converted into counts by convolution with the PSF and multiplying with the exposure. Systematic uncertainties are introduced in this analysis by the choice of the GALPROP model providing the templates to be fitted to the data. We study this effect in detail (see also [11] for a detailed study of different GALPROP models and comparisons with *Fermi*-LAT data).

3.2 *Fermi* Bubble Template

In order to define a template for the *Fermi* bubbles, we perform an all-sky fit with the templates listed above except the bubble template. Since no template accounts for the bubble flux a bias might be introduced by the other templates trying to compensate for the bubble flux. To avoid this we mask the region of interest in the fit. We define the region of interest as an ellipse centered in the Galactic center (see Fig. 1). Furthermore, point sources from the 2FGL catalog which have a TS value larger than 25 (i.e. a significance of 5σ) are masked with a radius of 1.48° which corresponds to the 95% containment region of the PSF at 1 GeV (see Fig. 2). All known extended sources are masked conservatively within a sphere with a radius corresponding to the sum of their major semi axes and the 95% PSF containment radius. Since the region of interest is masked the sources can not be fitted in that region.

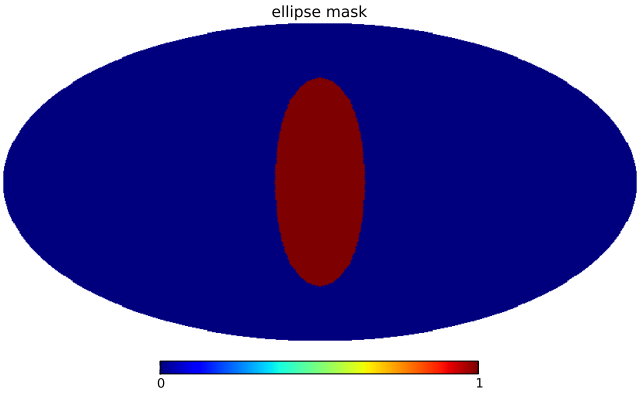

Fig. 1: Ellipse mask defining the region of interest, which is masked in the all-sky fit to avoid a bias created by other fit components compensating for the bubble flux.

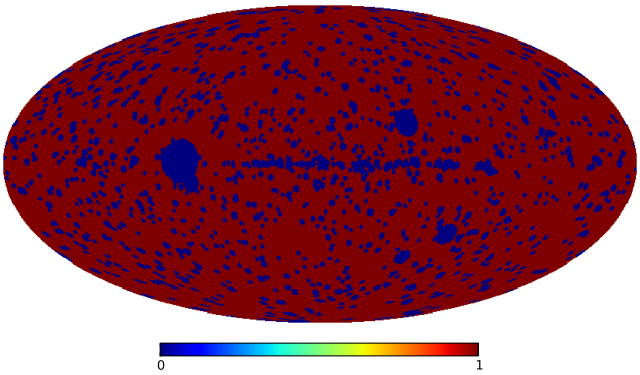

Fig. 2: Point source and extended source mask (sources with TS$>$ 25 are masked within a radius of 1.48°).

The bubble template is defined from the integrated significance map at energies 6.4 GeV $< E <$ 289.6 GeV smoothed with a Gaussian kernel of RMS $\sigma = 2^\circ$. The masked point sources are filled with an average of the neighboring non-masked pixels before the smoothing.

The defined template is then included in an all sky fit to obtain the spectrum of the bubble.

3.3 Results

We will show the overall spectrum of the *Fermi* bubbles and investigate a variation of the spectrum throughout the bubbles. Furthermore we will study the spatial morphology.

Acknowledgment: The *Fermi*-LAT Collaboration acknowledges support from a number of agencies and institutes for both development and the operation of the LAT as well as scientific data analysis. These include NASA and DOE in the United States, CEA/Irfu and IN2P3/CNRS in France, ASI and INFN in Italy, MEXT, KEK, and JAXA in Japan, and the K. A. Wallenberg Foundation, the Swedish Research Council and the National Space Board in Sweden. Additional support from INAF in Italy and CNES in France for science analysis during the operations phase is also gratefully acknowledged.

References

[1] M. Ackermann *et al.* [Fermi-LAT Collaboration], AIP Conf. Proc. **1085**, 763 (2009).
[2] A. A. Abdo *et al.* [Fermi-LAT Collaboration], Phys. Rev. Lett. **104**, 101101 (2010)
[3] I. V. Moskalenko and A. W. Strong, Astrophys. J. **493**, 694 (1998)
[4] A. W. Strong, I. V. Moskalenko and O. Reimer, Astrophys. J. **537**, 763 (2000) [Erratum-ibid. **541**, 1109 (2000)]
[5] V. S. Ptuskin, I. V. Moskalenko, F. C. Jones, A. W. Strong and V. N. Zirakashvili, Astrophys. J. **642**, 902 (2006)
[6] A. W. Strong, I. V. Moskalenko and O. Reimer, Astrophys. J. **613**, 962 (2004)
[7] T. A. Porter, I. V. Moskalenko, A. W. Strong, E. Orlando and L. Bouchet, Astrophys. J. **682**, 400 (2008)
[8] A. E. Vladimirov, S. W. Digel, G. Johannesson, P. F. Michelson, I. V. Moskalenko, P. L. Nolan, E. Orlando and T. A. Porter *et al.*, Comput. Phys. Commun. **182**, 1156 (2011)
[9] [Fermi-LAT Collaboration], Astrophys. J. Suppl. **199**, 31 (2012)
[10] K. M. Gorski, E. Hivon, A. J. Banday, B. D. Wandelt, F. K. Hansen, M. Reinecke and M. Bartelman, Astrophys. J. **622**, 759 (2005)
[11] [Fermi-LAT Collaboration], Astrophys. J. **750**, 3 (2012)
[12] M. Wolleben, Astrophys. J. **664**, 349 (2007)
[13] H. -Y. K. Yang, M. Ruszkowski, P. M. Ricker, E. Zweibel and D. Lee, Astrophys. J. **761**, 185 (2012)
[14] P. Mertsch and S. Sarkar, Phys. Rev. Lett. **107**, 091101 (2011)
[15] R. M. Crocker and F. Aharonian, Phys. Rev. Lett. **106**, 101102 (2011)
[16] M. Su, T. R. Slatyer and D. P. Finkbeiner, Astrophys. J. **724**, 1044 (2010)
[17] S. L. Snowden, R. Egger, M. J. Freyberg, D. McCammon, P. P. Plucinsky, W. T. Sanders, J. H. M. Schmitt and J. Truemper *et al.*, Astrophys. J. **485** (1997) 125.
[18] D. P. Finkbeiner, astro-ph/0409027.
[19] D. Pietrobon, K. M. Gorski, J. Bartlett, A. J. Banday, G. Dobler, L. P. L. Colombo, L. Pagano and G. Rocha *et al.*, Astrophys. J. **755**, 69 (2012)
[20] P. A. R. Ade *et al.* [Planck Collaboration], arXiv:1208.5483 [astro-ph.GA].
[21] F. Guo and W. G. Mathews, Astrophys. J. **756**, 181 (2012)
[22] E. Carretti, R. M. Crocker, L. Staveley-Smith, M. Haverkorn, C. Purcell, B. M. Gaensler, G. Bernardi and M. J. Kesteven *et al.*, Nature **493**, 66 (2013)
[23] Large *et al.*, MNRAS **124**, 405 (1962)